

## FORMATION OF DISSIPATIVE STRUCTURES IN GALAXIES

TOSHIYA NOZAKURA AND SATORU IKEUCHI

Department of Physics, Hokkaido University

Received 1983 May 16; accepted 1983 September 13

## ABSTRACT

A new idea that the spatial structures in various galaxies are regarded as “dissipative structures,” which are found in nonequilibrium and open systems, is presented. Fundamental physical processes in galaxies are mutual interchange processes among three components of the interstellar medium (ISM). First, the temporal behaviors (=time structures) of the ISM are investigated by a set of model equations. Second, adding the diffusion term to each component, we explore the physical mechanisms for the formation of spatial structures. We prove three different types of “dissipative structures” may appear in our ISM system. Third, the pattern formation is studied in a differentially rotating disk. It is shown that our idea is successful in the formation of spiral structures in galaxies. Finally, this result is compared with that of the stochastic self-propagating star formation model.

*Subject headings:* galaxies: evolution — galaxies: internal motions — galaxies: structure

## I. INTRODUCTION

In recent years, a new approach for investigating the origin of spiral structures in some galaxies has been developed. Its basis is that the star formation process propagates stochastically in a differentially rotating galaxy and the global structure of star forming regions is seen as a spiral arm (see Seiden and Gerola 1982 for a review). Therefore, this model is called the stochastic self-propagating star formation process (SSPSF). This is essentially different than the density wave theory, in which the gravitational potential of a galaxy plays the most important role in producing the global structure of star-forming regions (Lin and Shu 1964; Lin, Yuan, and Shu 1969; Roberts 1969).

It is notable that SSPSF has succeeded in explaining especially the irregular, patchy spiral structures (Gerola and Seiden 1978) which can not be understood by the density wave theory. Further, Cowie and Rybicki (1982) claimed that the hypothesis of self-propagating star formation can lead to a regular solitary wave pattern in a differentially rotating galaxy. In these ideas, the sequential star formation process (Elmegreen and Lada 1977) is assumed and modeled uniquely. In SSPSF, the star formation process is replaced by a stochastic process, so that the relation between the local star formation process and the global spatial structure is not physically unambiguous. In the latter model, the propagation of star formation is treated as a wave from the outset.

In the present paper, we propose a new model for the formation of global structure in galaxies. It is based upon the viewpoint that the global spatial structure of a galaxy is produced by the local physical process and its propagation. In other words, the galactic structure can be regarded as a special example of “dissipative structures/self-organized structures.”

The concept of “dissipative structures” has been extensively developed for the past decade (Nicolis and Prigogine 1977). Their typical examples are found in the pattern formation phenomena in chemically reacting systems. In some chemical

reactions, beautiful and mysterious concentration patterns like those shown in Figure 1 appear in certain experimental conditions (Winfree 1974a). These phenomena can be analyzed by using a set of equations of the form

$$\begin{aligned} \frac{\partial X}{\partial t} &= F(X) + \tilde{D} \nabla^2 X, \\ X &= (X_1, \dots, X_N)^T, \\ \tilde{D} &= \begin{vmatrix} D_1 & \dots & 0 \\ 0 & \ddots & \\ 0 & & D_N \end{vmatrix}, \end{aligned} \quad (1.1)$$

where  $X_i = X_i(r, t)$  is the concentration of  $i$ th reactant,  $D_i$  is its diffusion coefficient, and  $r$  and  $t$  are the spatial and time coordinate, respectively. The first term  $F(X)$  of the right-hand side represents chemical reactions, and the second term  $\tilde{D} \nabla^2 X$  represents the spatial diffusion. In short, the essential part of the method of “dissipative structures” is how the spatial and time structures of reactants can be derived from a set of equations like (1.1) (Nicolis and Prigogine 1977).

In the present case, we want to see how the spatial distributions of H II regions are formed in a galaxy, because they are the most prominent tracers of spiral arms. Since the massive stars which are illuminating the H II regions are born from the cold gas component of interstellar medium (ISM), the fundamental physical processes in a galaxy are the mutual interchange processes in ISM.

We take a simple model for them (Ikeuchi and Tomita 1983): The interstellar medium is composed of three components, i.e., cold clouds ( $T_c \lesssim 10^2$  K,  $n_c \gtrsim 10$  cm<sup>-3</sup> with subscript  $c$ ), hot gas ( $T_h \gtrsim 10^6$  K,  $n_h \lesssim 10^{-2}$  cm<sup>-3</sup> with subscript  $h$ ) and warm gas ( $T_w \sim 10^4$  K,  $n_w \lesssim 1$  cm<sup>-3</sup> with subscript  $w$ ), and they are transformed to each other driven by supernova (SN) explosions. Mutual interchange processes are shown schematically in Figure 2, and each simplified process is described in § II. We call them cyclic phase change processes of ISM.

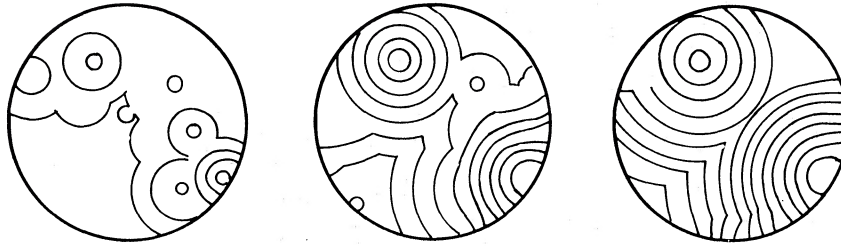


FIG. 1.—An example of concentration patterns appeared in Belousov-Zhabotinsky reaction in a thin petri dish (from the photograph by Winfree (1974a))

Apparently, our approach is quite different from that of SSPSF. The principal purpose of this paper is to reveal that the concept of “dissipative structure” can successfully make clear the relation between the local (nonlinear) physical processes and the global spatial structures of a galaxy such as the relation between the local star formation process from interstellar clouds and the spiral structure. Therefore, we do not take care of the quantitative accuracy at present but emphasize this approach to be powerful.

A work similar to the present paper was recently published (Shore 1983). In that work, considering a galaxy to be composed of stars and interstellar gas and examining their mutual interchange processes, Shore (1983) discussed the possibility for the formation of spatial structures. However, he could not present any clear conclusions because his analysis was limited to the usual linear and analytical treatment.

In § II, the basic equations are presented. In § III, the time structures of the ISM are derived from basic equations. In §§ IV and V, the numerical results of spatial structures when the diffusion terms are included as in equation (1.1) are shown. The differential rotation is considered in § V. In § VI, our results are summarized in comparison with SSPSF model, and some comments are added.

## II. BASIC EQUATIONS

### a) Interchange Processes in ISM

As the local physical processes, which correspond to the nonlinear terms in equation (1.1), we consider the mutual interchange processes in ISM. “Local” means that the linear dimension considered is of the order of several hundreds of parsecs, within which one supernova can complete its life (Chevalier 1974).

The mutual interchange processes of ISM were extensively explored (Habe, Ikeuchi, and Tanaka 1981; Ikeuchi, Habe, and

Tanaka 1984). But they are too complicated to examine the global structures. Here, following the work by Ikeuchi and Tomita (1983), we use a set of simplified model equations which qualitatively reproduce the temporal behavior of cyclic phase change of ISM. The basic equations are as follows (Ikeuchi and Tomita 1983):

$$\frac{dX_c}{dt} = AX_w - BX_cX_h^2, \quad (2.1a)$$

$$\frac{dX_h}{dt} = BX_cX_h^2 - X_hX_w, \quad (2.1b)$$

$$\frac{dX_w}{dt} = X_hX_w - AX_w, \quad (2.1c)$$

where  $X_i$ 's ( $i = c, h, w$ ) are the local masses of three components, and  $A$  and  $B$  are the positive coefficients of interchange rates.

The above set of basic equations is a simplified form of interchange processes shown in Figure 2. Although each process is to depend upon the temperature, supernova rate, and filling factors, we effectively absorb them into the functional form of each term and into the constant parameters  $A$  and  $B$ . The sweeping rate of warm ambient gas by SN shells is written as  $AX_w$ , because we know (Habe, Ikeuchi, and Tanaka 1981) that the final sweeping rate is relatively insensitive to the temperature and density of ambient gas. The term  $BX_cX_h^2$  expresses the evaporation rate of cold clouds embedded in hot gas. In order to represent that evaporation rate depends sensitively upon the temperature of hot gas ( $T^{5/2}$ ; Spitzer 1962), we express the evaporation rate with the highest nonlinearity of  $X_h^2$ . The cooling rate of hot gas to warm component is expressed as  $X_hX_w$ .

At first sight, the above model equations seem to be a too rough approximation. However, as is seen in the following section and the paper by Ikeuchi and Tomita (1983), they

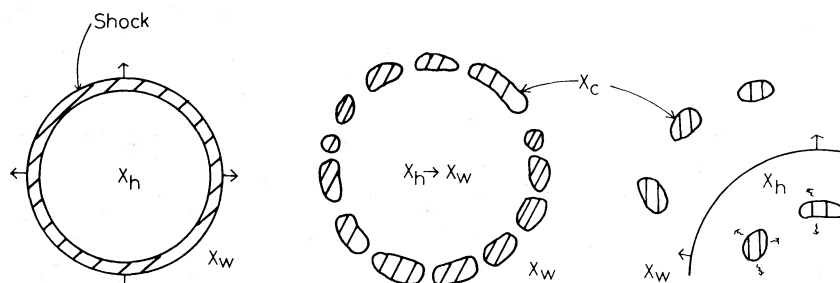


FIG. 2.—Schematic representation of mutual interchange processes of ISM. (left) A warm ambient gas is swept by the SN shell. (center) A hot gas in the SN cavity cools to a warm gas. (right) Cold clouds made through the shell destruction are evaporated within a hot gas of a new SN cavity.

qualitatively reproduce the temporal behavior of the ISM fairly well. Therefore, we may start the investigation from the above model equations.

### b) Spatial Interactions of Local Processes

For the study of the structure of ISM on a galactic scale, we must include the spatial interaction and/or spatial propagation of local processes. Here, we assume that the mass flux of the  $i$ th component can be described as  $S_i = -D_i \partial X_i(r, t) / \partial r$ , where  $D_i$  is the constant coefficient. Similar to thermal conduction, **this expression means that each component flows from the place where it is rich to the place where it is poor.** We believe that this is the most natural expression for the mass flow. For example, the random motion of clouds is exactly expressed as this form, and the coefficient

$D_c$  has the meaning,  $D_c \equiv (\text{mean random velocity})^2 \times (\text{mean free time})$  (Landau and Lifschitz 1959). Taking these transporting terms into account, a set of equations leads to the following:

$$\frac{\partial X_c}{\partial t} = AX_w - BX_c X_h^2 + D_c \nabla^2 X_c, \quad (2.2a)$$

$$\frac{\partial X_h}{\partial t} = BX_c X_h^2 - X_h X_w + D_h \nabla^2 X_h, \quad (2.2b)$$

$$\frac{\partial X_w}{\partial t} = X_h X_w - AX_w + D_w \nabla^2 X_w, \quad (2.2c)$$

where each component  $X_i$  ( $i = c, h, w$ ) depends upon the time  $t$  and space  $r$  coordinates.

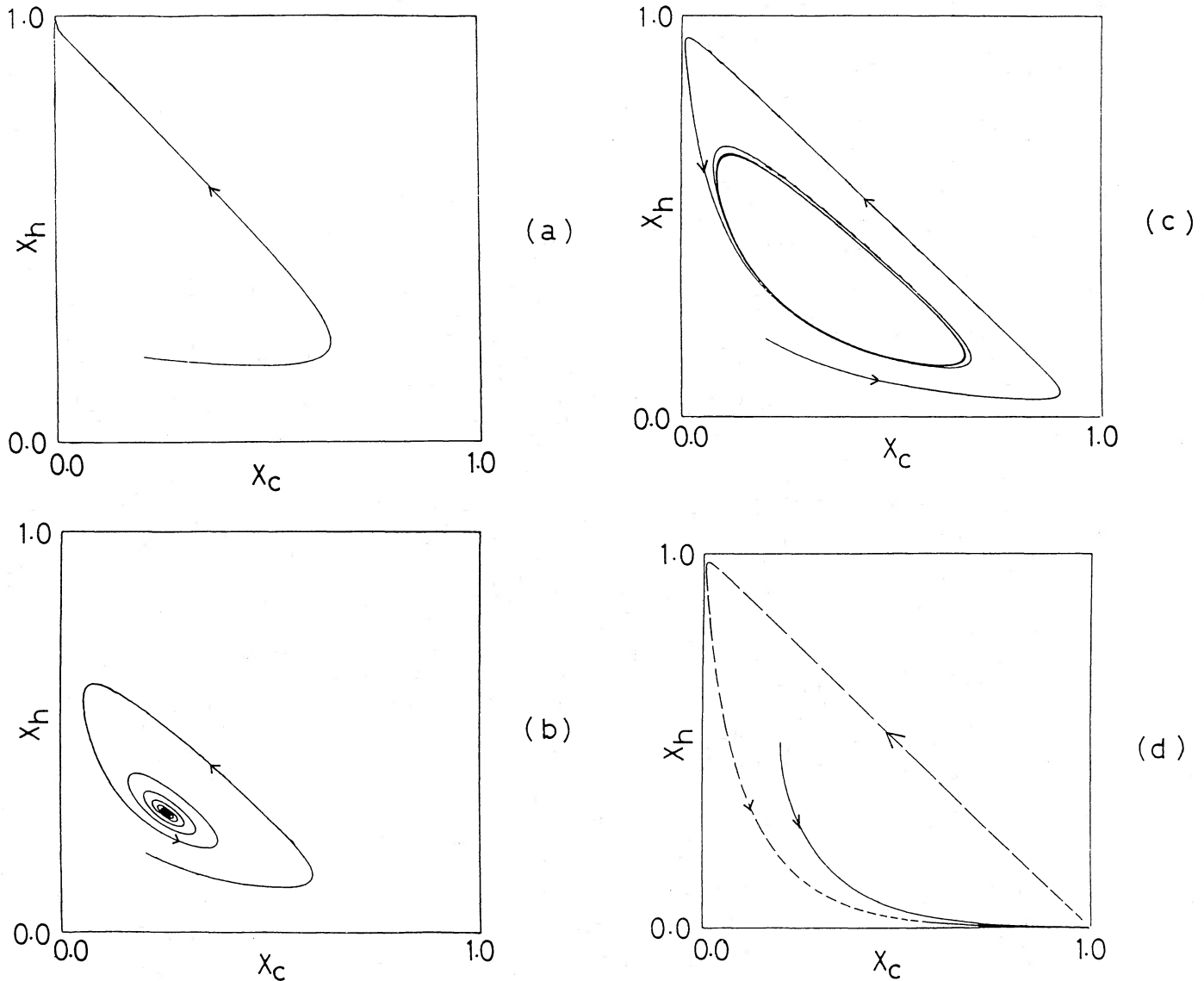


FIG. 3.—Four qualitatively different temporal behaviors of ISM. The adopted parameters are (a)  $A = 1.2$ ,  $B = 4.0$ ; (b)  $A = 0.3$ ,  $B = 6.0$ ; (c)  $A = 0.3$ ,  $B = 3.0$ ; and (d)  $A = 0.15$ ,  $B = 1.0$ . In case (d), the system is captured to Cold Phase for a very long time (full line). Eventually it escapes from there and follows a large circuit (dashed line).

## III. TIME STRUCTURE OF INTERSTELLAR MEDIUM

Before going to the formation of spatial structure of ISM in a galaxy, we briefly summarize the time structure—temporal behavior—of the ISM (Ikeuchi and Tomita 1983; Ikeuchi, Habe, and Tanaka 1984). Since equation (2.1) is a conservative system, we normalize the total mass unity, i.e.,  $X_c + X_h + X_w = 1$  and describe the set of three stationary states (1), (2), and (3) as  $(X_c^0, X_h^0)$ , which are

$$(1) (1, 0) \text{ and } (2) (0, 1) \text{ when } A > 1, \quad (3.1)$$

$$(1), (2), \text{ and } (3) \left( \frac{1-A}{1+BA}, A \right) \text{ when } A < 1. \quad (3.2)$$

Equation (2.1) has four qualitatively different types of temporal behavior depending upon the parameters  $A$  and  $B$ . They are shown in Figure 3.

*Figure 3a.*—If  $A > 1$ , the system monotonically approaches the stationary state (2) as in Figure 3a, that is, the ISM becomes entirely hot. This result is already confirmed in the work by Ikeuchi, Habe, and Tanaka (1984) when SN rate is sufficiently high.

*Figure 3b.*—If  $A < 1$  and  $B > B_c \equiv (1-2A)/A^2$ , the stationary state (3) is a stable focus as in Figure 3b. This corresponds to the steady two-phase (Field, Goldsmith, and Habing 1969) or three-phase model (McKee and Ostriker 1977) of the ISM which are obtained for an appropriate SN rate.

*Figure 3c.*—If  $A < 1$  and  $B < B_c$ , the orbit in  $X_c - X_h$  plane asymptotically approaches a “limit cycle” (Minorsky 1962) as in Figure 3c. This behavior is also obtained as the solution which periodically undergoes cold phases and hot phases in turn in the case of a moderately high SN rate.

*Figure 3d.*—If  $A \ll 1$  and  $B \ll B_c$ , this is the extreme case of the above limit cycle solution. Since the system stays near cold phase, i.e., near  $(1, 0)$ , for a very long time as in Figure 3d (full line), the system is practically captured to cold phase forever. Physically, the coefficient  $A$  of the sweeping term is so small that the system stays long in an entirely cold phase. Considering that the system eventually escapes from cold phase and draws a cycle in the phase plane (dashed line), its temporal behavior can be regarded as an extreme example of relaxation oscillation.

Since the above-mentioned three cases (a), (b), and (c) qualitatively reproduce the three types of solutions in the work by Ikeuchi, Habe, and Tanaka (1984), equation (2.1) proves to be a good approximation for the “cyclic phase change processes of ISM.” The detailed discussion about the physical meanings of the above solutions are given in Ikeuchi and Tomita (1983).

Finally, we would like to note that the above temporal behavior of the ISM is easily proven by the linear stability analysis of equation (2.1) (Minorsky 1962). This is the great advantage of our method starting from model equations.

## IV. THREE TYPES OF PHYSICAL MECHANISMS OF PATTERN FORMATION

It is generally known (Winfree 1978) that such an equation as (2.2) can have three different types of physical mechanisms for the formation of spatial structures depending upon the nonlinear reaction terms  $F_i$  and the diffusion coefficients  $D_i$ . As is shown in the following, equation (2.2) has all three types of pattern formation caused by introducing diffusion processes

to the time structure cases (b), (c), and (d) above. [As the time structure (a) leads to a physically meaningless state, i.e.,  $X_i < 0$ , we do not examine it.]

## a) Symmetry Breaking Type

We consider the case that equation (2.1) has a stable stationary state of type (b), and that the system is in the uniform stationary state,

$$X_c^0 = \frac{1-A}{1+BA}, \quad (4.1a)$$

$$X_h^0 = A, \quad (4.1b)$$

$$X_w^0 = 1 - X_c^0 - X_h^0. \quad (4.1c)$$

When the diffusion terms are included, this stationary state (4.1) could become unstable for appropriate values of  $D_c$ ,  $D_h$ , and  $D_w$ . In that case, some unstable mode pattern in the distribution of components grows from an arbitrary initial perturbation to another stationary state, in which the nonlinear terms balance the diffusion terms. As a result, a nonuniform, steady distribution of ISM is obtained.

This type of spatial structure is called “symmetry breaking type,” because a structure with lower spatial symmetry than the uniform stationary state appears. The final spatial pattern is determined by the parameters  $A$ ,  $B$ ,  $D_c$ ,  $D_h$ , and  $D_w$  as well as the boundary condition, and does not depend on the shape of initial perturbation. That is, the system can have a global spatial structure, which depends only on the local physical processes ( $A$ ,  $B$ ,  $D_c$ ,  $D_h$ ,  $D_w$ ).

It seems curious at first sight that the uniform stationary state becomes unstable when diffusion processes are introduced. The reason why this instability appears had been given by Turing (1952). In short, when diffusion terms are added, the linearized equations for infinitesimal perturbations of a particular mode change to those with effectively different coefficients  $A$  and  $B$ , and the stable uniform state may be enforced into an unstable one in some cases. In other words, the mass flow due to the diffusion term of one component may bring a perturbation into another component, which grows under a certain circumstance. Therefore it is easily shown that the following two conditions, at least, are necessary for the appearance of “symmetry breaking type” instability. One is that more than two components must be mutually interacting. The other is that all the diffusion coefficients must not be equal. Apparently, both of them are satisfied in our equation (2.2).

We can show by the usual linear analysis when a mode becomes unstable. In the present case of an infinitesimally thin disk (galactic disk), the eigenmodes of the Laplacian are given by the Bessel functions, i.e.,

$$\nabla^2 [\cos(m\theta)J_m(kr)] = -k^2 [\cos(m\theta)J_m(kr)], \quad (4.2)$$

where  $r$  and  $\theta$  are the radial and the angular coordinates on the disk. Then, the perturbations from the uniform stationary state (4.1) are assumed to be the form

$$x_i = A_i e^{\omega t} \cos(m\theta)J_m(kr), \quad (4.3)$$

and they are substituted into the linearized equations of (2.2). After some calculation, we get the dispersion relation

$$\omega^3 + \omega^2 p + \omega q + r = 0, \quad (4.4)$$



where  $p$ ,  $q$ , and  $r$  are the functions of  $k^2$ ,  $A$ ,  $B$ ,  $D_c$ ,  $D_h$ , and  $D_w$ . We can see the stability of a given mode from this dispersion relation (cf. Hershkowitz-Kaufman and Nicolis 1972).

In Figure 4, an example of the structure due to "symmetry breaking type" instability is shown. Parameters are set so as for the  $J_0(8.65r/R)$  mode to become unstable. The abundance of cold component reaches asymptotically a steady value. In Figure 4b, the final steady structure which resembles to the function  $J_0(8.65r/R)$  is shown.

Perhaps this example may not be realistic because the result depends on the boundary condition. However, the above-mentioned physical mechanism for the formation of spatial structures will be valid irrespective of the boundary conditions.

#### b) Phase Wave Type

We consider the case that equation (2.1) has a periodic state of type (c), i.e., "limit cycle." If diffusion processes are taken into account, the following structure is expected (Ortoleva and Ross 1973). At each spatial point  $r$ , the ISM

system behaves like the original limit cycle, but the phase is slightly different at each point. Diffusion terms act so as to adjust the phase difference of neighbors, and consequently the phase will propagate as a progressive wave. The presence of such a "phase wave type" structure is described as the following theorem (Kopell and Howard 1973): Suppose that  $F(X)$  in equation (1.1) has a stable limit cycle solution. Then, the diffusion-included equation (1.1) has a one-parameter family of periodic wave solutions of the form

$$X_i = X_i(\omega t - \mathbf{k} \cdot \mathbf{r}). \quad (4.5)$$

If we assign one parameter  $k \equiv |\mathbf{k}|$  (or  $\omega$ ), the angular frequency  $\omega$  (or the wave number  $k$ ) and the wave form are determined uniquely. The long wavelength limit ( $k \rightarrow 0$ ) just corresponds to the original uniform limit cycle with no phase difference.

Assuming that the wave form is that of equation (4.5), we construct a family of  $2\pi$  periodic solutions for our equation (2.2). Here, we set  $D_c = D_h = D_w = D$  for simplicity and take the input parameter as  $\beta \equiv Dk^2/\omega^2$ . In Figure 5, we show two

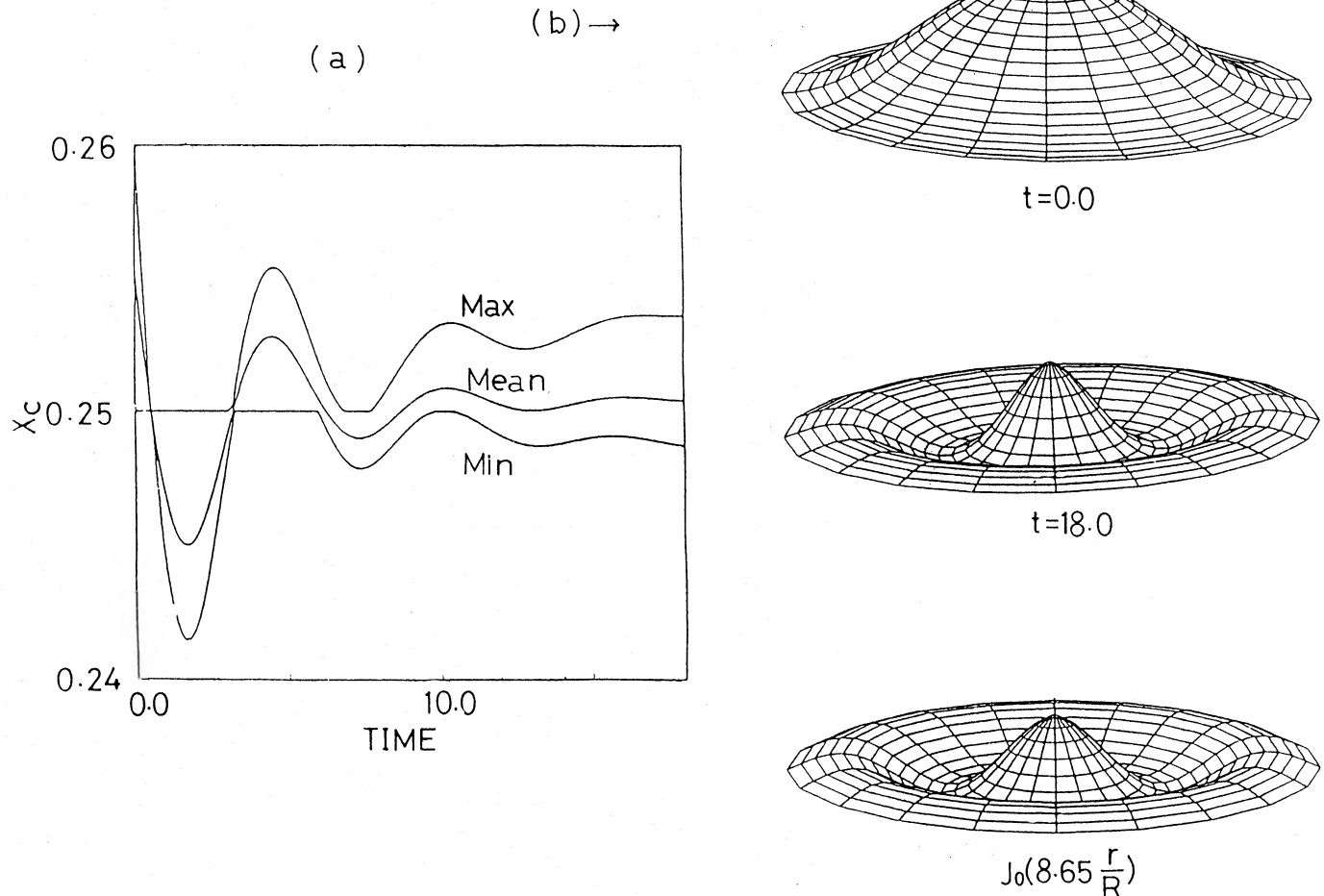


FIG. 4.—A "Symmetry Breaking Type" structure. Parameters are  $A = 0.3$ ,  $B = 6.0$ ,  $D_c = 0.05$ ,  $D_h = 0.005$ ,  $D_w = 0.05$ , and  $R = 8.65$ . Fixed boundary conditions, i.e.,  $X_i(R, \theta, t) = X_i^0$ , are taken. In (a), the time variation of abundances of cold component for the maximum and minimum points is shown. Its mean abundance on the two-dimensional disk is also shown. In (b), the initial perturbation ( $t = 0$ ) and final steady distribution ( $t = 18.0$ ) of cold component are shown. Plotted is the difference from the uniform stationary state, i.e.,  $X_c(r, \theta, t) - X_c^0$ , by a proper scaling. Also, the function  $J_0(8.65r/R)$  is shown for comparison.

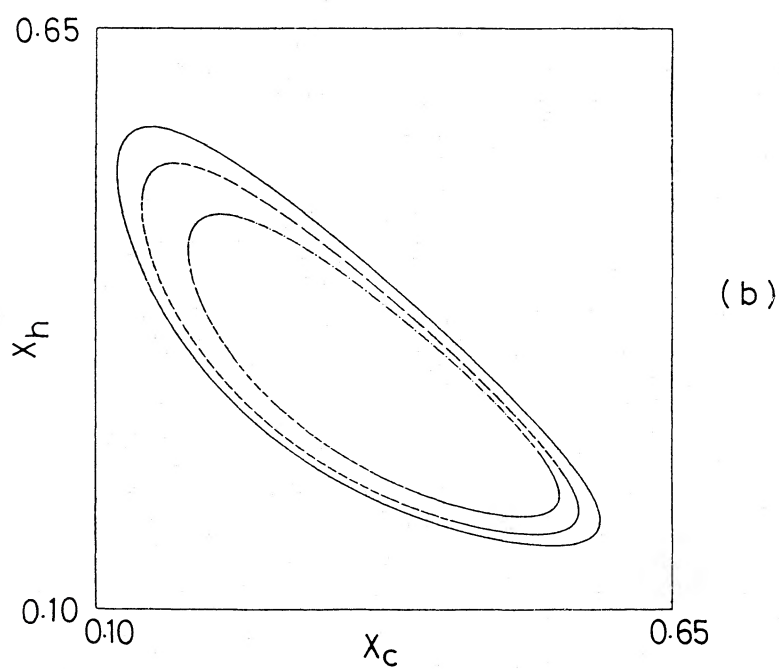
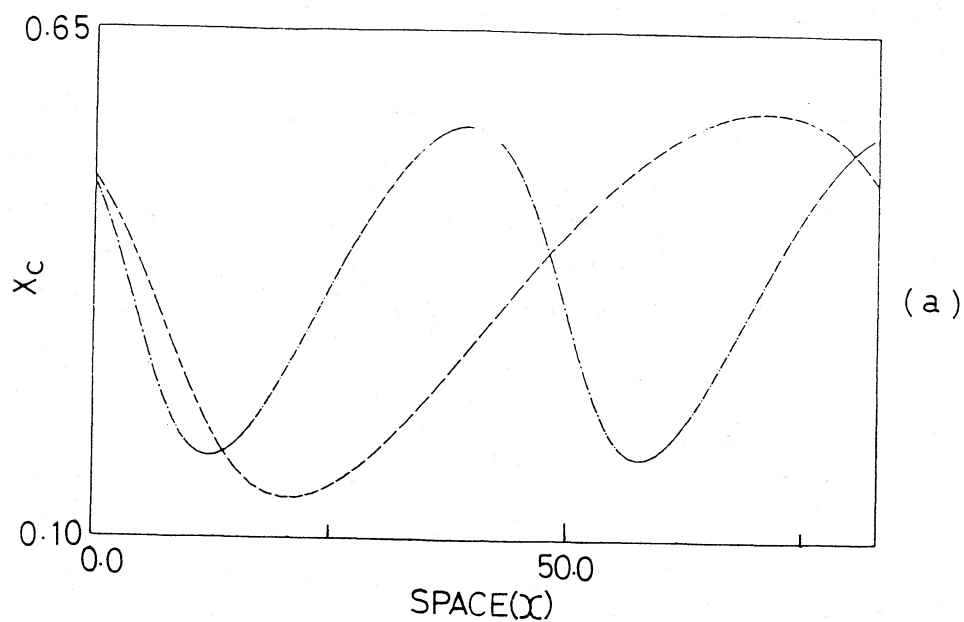


FIG. 5.—An example of the family of “Phase Wave Type” structure. Parameters are  $A = 0.3$ ,  $B = 3.5$ , and  $D_c = D_h = D_w = D$ . Two members with different  $\beta (\equiv Dk^2/\omega^2)$ , i.e.,  $\beta = 0.03$  (dashed lines) and  $0.09$  (dash-dotted lines), are shown. (a) Wave profiles of cold component  $X_c(\omega t - kx)$  for a fixed time. (b) Projections of their one wavelength portion onto the  $X_c - X_h$  phase plane. The uniform limit-cycle solution ( $\beta = 0.0$ ) is also plotted by a solid line.

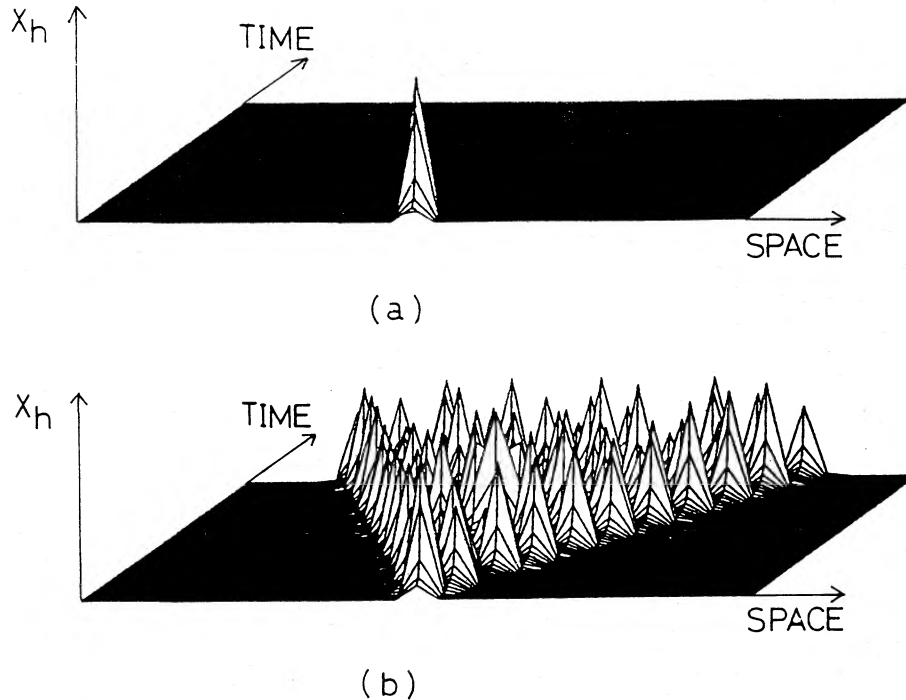


FIG. 6.—One-dimensional “Trigger Wave” structure. Parameters are taken as  $A = 0.15$ ,  $B = 1.0$ , and  $D_c = D_h = D_w = D$ . Initial perturbations are given at the center as (a)  $D = 0$  and (b)  $D = 10^{-3}$ . Trigger wave does not appear in (a), and it propagates in (b) because of moderately large diffusion coefficients.

members with different  $\beta$  in such a family of solutions. Figure 5a shows wave trains for a fixed time, and Figure 5b shows the projections of their one wavelength portion onto the  $X_c - X_h$  phase plane.

In this “phase wave type,” a particular solution is not obtained by a simulation from an arbitrary initial perturbation, because for a sufficiently small  $\beta$  all the members of the family can appear equally (Kopell and Howard 1973), so that there are no reasons for a particular member to dominate.

### c) Trigger Wave Type

As in Figure 3d, we consider the case that the ISM system described by equation (2.1) is captured to the  $(X_c^0, X_h^0) = (1, 0)$  state (cold phase) and never escapes from there. However, if a certain perturbation whose magnitude is more than the threshold is given, then the system responds to it, follows a large circular orbit in the phase plane and returns to cold phase again as shown by a dashed line. Systems having such a nature are called “excitable systems” (Winfree 1974b; Greenberg, Hassard, and Hastings 1978).

If there are no diffusion terms, any initial distributions disappear after a sufficiently long time and everywhere goes to the same cold phase as shown in Figure 6a. However, if diffusion coefficients are moderately large, the perturbation at an arbitrary place triggers the neighbors from cold phase to hot phase. This triggering effect propagates in succession. As a result, the “trigger wave” propagates as in Figure 6b, where the amount of hot gas component  $X_h(r, t)$  is illustrated. Generally, the wave velocity depends upon the diffusion coefficients  $D_c$ ,  $D_h$ , and  $D_w$ , while the wave amplitude is independent of them, i.e.,  $X_h \sim 1$  as long as they are not so large. Once the wave spreads out through the entire space,

there always exist some kinds of stationary waves, that is, the ISM system at each point behaves like a relaxation oscillation.

The spatial structure obtained from this “trigger wave type” clearly resembles to that of SSPSF. Comparison of these two models is described in § VI.

At the end of this section, it should be noted that the principal physical basis for the above-mentioned three types of spatial structures can be inferred from the time structures, “stable stationary state,” “limit cycle,” and “excitable system,” regardless of the explicit form of nonlinear terms. Therefore, if there are any other systems which show similar temporal behaviors, the same spatial structures as the above can be expected to appear in them. Consequently, even if the details of equation (2.2) are revised in the future, so far as the qualitative nature of the time structure is unchanged, the above results are also unchanged.

### V. EFFECTS OF DIFFERENTIAL ROTATION

So far we have not considered the differential rotation of a galactic disk. In this section we take it into account under the assumption that the ISM is rotating at an angular velocity  $\Omega(r)$ . Then equations become

$$\frac{\partial X_c}{\partial t} + \Omega(r) \frac{\partial X_c}{\partial \theta} = AX_w - BX_c X_h^2 + D_c \nabla^2 X_c, \quad (5.1a)$$

$$\frac{\partial X_h}{\partial t} + \Omega(r) \frac{\partial X_h}{\partial \theta} = BX_c X_h^2 - X_h X_w + D_h \nabla^2 X_h, \quad (5.1b)$$

$$\frac{\partial X_w}{\partial t} + \Omega(r) \frac{\partial X_w}{\partial \theta} = X_h X_w - AX_w + D_w \nabla^2 X_w, \quad (5.1c)$$

where each component depends upon  $r$ ,  $\theta$ , and  $t$ .

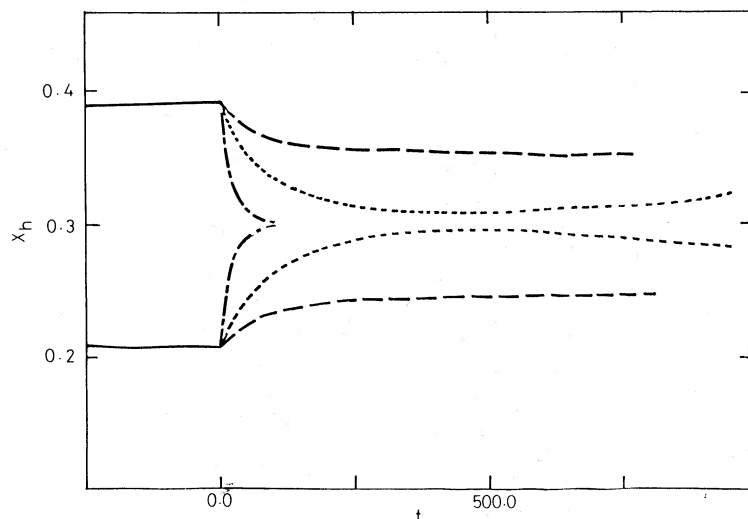


FIG. 7.—Effects of differential rotation on “Symmetry Breaking Type” structure. The time variations of abundances of hot component for the maximum and minimum points on the two-dimensional disk are shown. At  $t = 0$ , the differential rotation is inserted with three different cases of  $\Omega_1$ , i.e.,  $\Omega_1 = 0.314$  (dashed line), 0.471 (dotted line), and 3.14 (dash-dotted line). Other parameters are the same as in Fig. 4.

As for the rotation law, we take the flat rotation curve for simplicity, i.e.,  $\Omega(r) = \Omega_1(r_1/r)$ , where  $\Omega_1$  is the angular velocity at the innermost mesh  $r = r_1$ .

In what follows, we examine the effects of differential rotation on the two types of structures “symmetry breaking type” and “trigger wave type.” Since the structures of “phase wave type” are not obtained by simulations, we are not concerned with it here.

#### a) Effects on “Symmetry Breaking Type” Structures

The calculation is done in the following way: In the first place, we set  $\Omega(r) = 0$  for all  $r$ , and a steady spatial structure is constructed by numerical integration of equation (2.2). Adopting this structure as the initial ( $t = 0$ ) condition, we follow the change in it when differential rotation  $\Omega(r)$  is included. This calculation method is taken for computational convenience, because it is difficult to construct a clear pattern when a system begins rotating differentially. Therefore, it is not certain that the clear patterns shown in the below can be found in realistic galaxies.

The growing manner of the initial spatial structure of “symmetry breaking type” is shown in Figure 7, where the numerical values of parameters are taken so as for the  $J_1(7.01r/R) \cos(\theta)$  mode to appear. In this set of parameters, the  $J_4(7.59r/R) \cos(4\theta)$  mode is also expected, but the former growing rate is much higher than the latter one. Then, the spatial structure resembling the  $J_1$  mode is set at the time  $t = 0$ .

At  $t > 0$ , we insert the differential rotation term with three cases of  $\Omega_1$ . As illustrated in Figure 7 and Figures 8a, 8b, and 8c, the spatial structure shows a mode transition depending upon the rotation rate.

Figure 8a.—At  $\Omega_1 = 0.314$ , in which the matter at the radius  $r$  rotates 0.125 ( $R/r$ ) times around the center during the time interval  $\Delta t = 50.0$ . The initial spatial structure is slightly distorted at first, but it begins to rotate rigidly keeping the original shape. The amplitude of spatial distribution gradually decreases, and finally a new steady structure is

established, which is rigidly rotating. The angular velocity of the pattern is nearly equal to that of the matter at the radius  $r = R/5$ .

Figure 8b.—At  $\Omega_1 = 0.471$ . The amplitude of the  $J_1$  mode decreases and gradually bifurcates to the new  $J_4(7.59r/R) \cos(4\theta)$  mode. After this “mode transition,” the amplitude of the  $J_4$  mode begins to increase, and it finally attains a quasi-steady value around which it fluctuates a little. This pattern is also rotating rigidly with the same angular velocity as the matter at  $r = R/4$ .

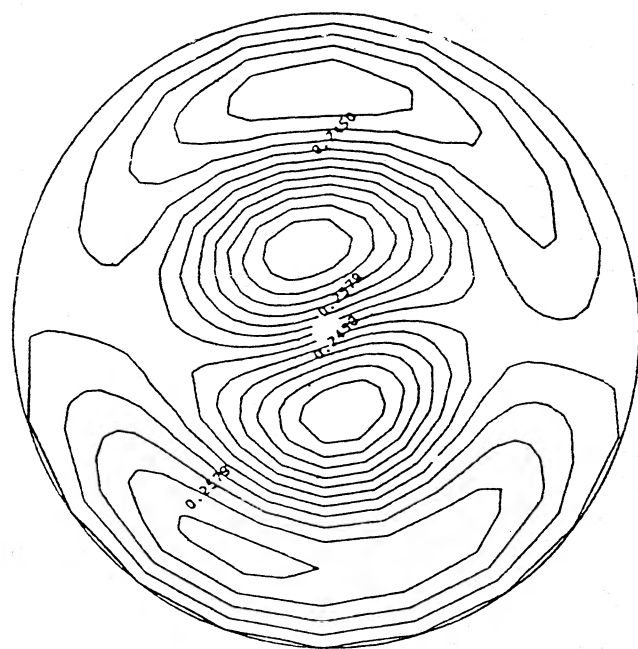
Figure 8c.—At  $\Omega_1 = 3.14$ . The amplitude of the initial  $J_1$  mode decreases rapidly and disappears, and the  $J_4$  mode does not appear.

The reason for the above “mode transition” is understood as follows. Figure 9 shows the radial changes of the  $J_1$  and  $J_4$  modes. As is seen, the  $J_4$  mode is more flattened than the  $J_1$  mode near the center ( $r \sim 0$ ). Since the effect of differential rotation is strong near the center [ $d\Omega(r)/dr \propto -r^{-2}$ ], the  $J_1$  mode is more easily twisted by the differential rotation than the  $J_4$  mode. At a relatively low differential rotation (a), the  $J_1$  mode can survive with a smaller amplitude than that for the case without differential rotation. With increasing the speed of differential rotation, the  $J_1$  mode is destroyed in the first place. Consequently, only the  $J_4$  mode can survive at a moderately high differential rotation and it grows in place of the  $J_1$  mode (b). Further increasing the speed as (c), the  $J_4$  mode is also destroyed soon.

From the above, we conclude that (1) the steady mode pattern changes according to the speed of differential rotation, and the mode with a flat structure near the center (or the place of the highest degree of differential rotation) can survive even at a moderately high speed; and (2) the fundamental mode is slightly distorted, but rotates rigidly, although the physical mechanism of “rigid rotation” of pattern is not clear at present.

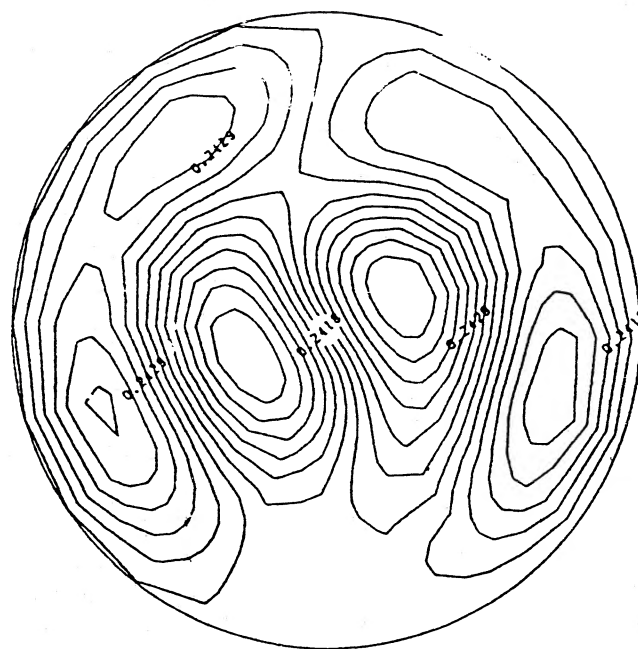
It is highly probable that various spatial structures observed in real galaxies may be interpreted as different mode patterns of “symmetry breaking type” depending upon their relative





$t=400.0$

FIG 8a



$t=200.0$

FIG. 8.—Contour maps of cold component for three cases in Fig. 7. (a) For  $\Omega_1 = 0.314$ , slightly distorted but rigidly rotating  $J_1$  mode is established. (b) For  $\Omega_1 = 0.471$ , the mode transition from  $J_1$  to  $J_4$  is clearly seen. (c) For  $\Omega_1 = 3.14$ , any clear mode does not appear.

strength among differential rotation, diffusion processes, and local physical processes.

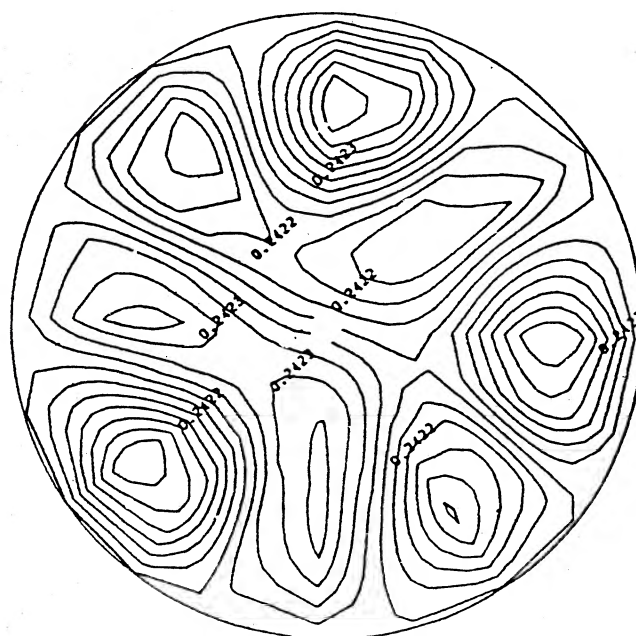
#### b) Effects on “Trigger Wave Type” Structures

Adopting the same parameters  $A$ ,  $B$ ,  $D_c$ ,  $D_h$ , and  $D_w$  as the case of one-dimensional trigger wave shown in Figure 6, we calculate the change of spatial patterns for three cases of differential rotations. Initially, two different perturbations are set at nearly symmetric places with respect to the center. The general tendencies of the results are summarized as follows.

1. In Figure 10, we compare the manner of propagations of trigger waves for three cases of rotation rates. As is seen, the higher the differential rotation is, the faster the trigger wave propagates and the more widely spread the triggered region is at the stage when the global structure reaches a kind of steady state. This means that the differential rotation effectively raises the diffusion rate.

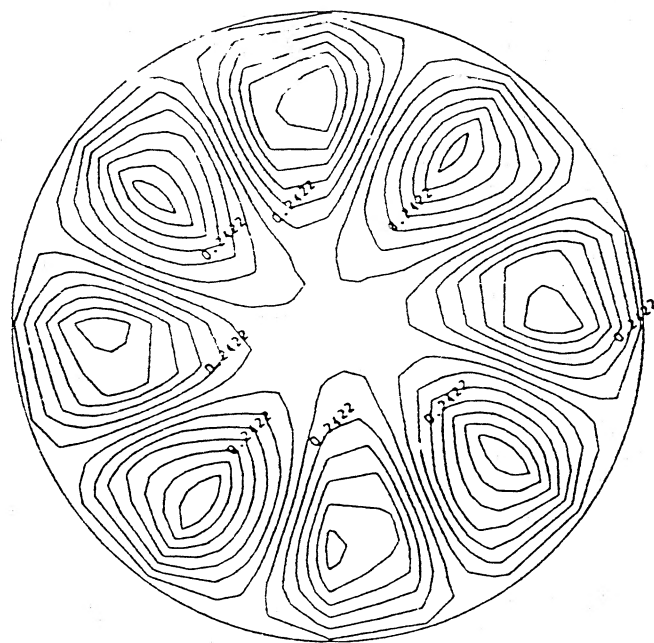
2. Under an appropriate rate of differential rotation, irregular, patchy but connected spiral structures are seen.

3. This spiral structure is considered to be a kind of steady pattern since similar structures are observed at any time. It is to be noted that this pattern is not wound up in the course of time. This means that the spiral arms are travelling on the disk. In other words, they are not the matter arms but the wave arms, the same as the rigidly rotating patterns of “symmetry breaking type.”



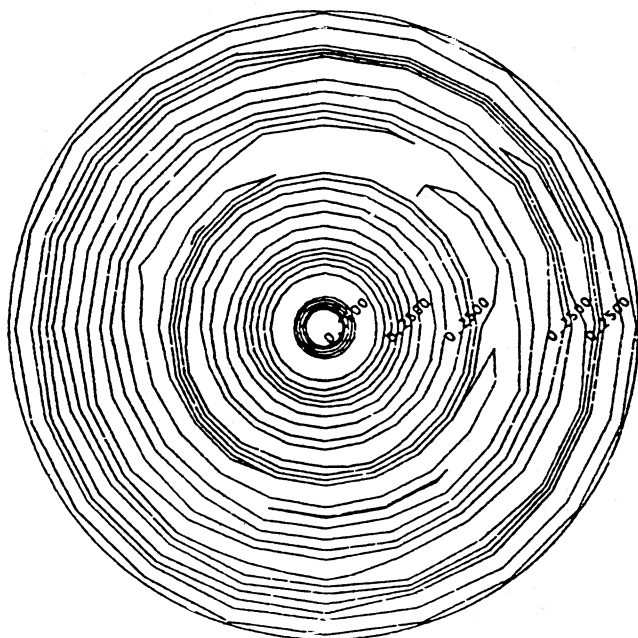
$t=400.0$

FIG. 8b



$t = 600.0$

FIG. 8b—Continued



$t = 150.0$

FIG. 8c

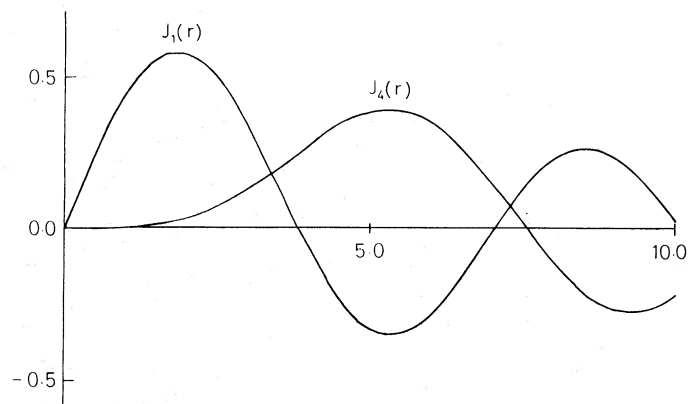


FIG. 9.—Bessel functions  $J_1(r)$  and  $J_4(r)$ . Near the center ( $r \sim 0$ ),  $J_4$  is more flattened than  $J_1$ .

As described in § IVc the physical nature of this trigger wave resembles that of SSPSF, so that the same relation between the spatial structure and the rotation strength is expected to hold. In fact, the above results (1) and (3) are also confirmed in SSPSF. Also, the solitary wave found by Cowie and Rybicki (1982) is a trigger wave.

Within the results obtained so far, we do not emphasize that our model is intrinsically superior to the SSPSF model in producing connected arms or string structures in spiral galaxies. There are two adjusting parameters in the SSPSF model, and by selecting parameter values properly the star-forming regions are guaranteed to connect in one direction.

In our model, since the recovery time, which is determined by the parameters  $A$  and  $B$ , is generally short in comparison with the rising time, which is the time needed for a system to respond to triggering perturbation, it is difficult to form a wave propagating in one direction. Therefore, irregular and patchy but connected arms are found only in a restricted range of the rotation speed.

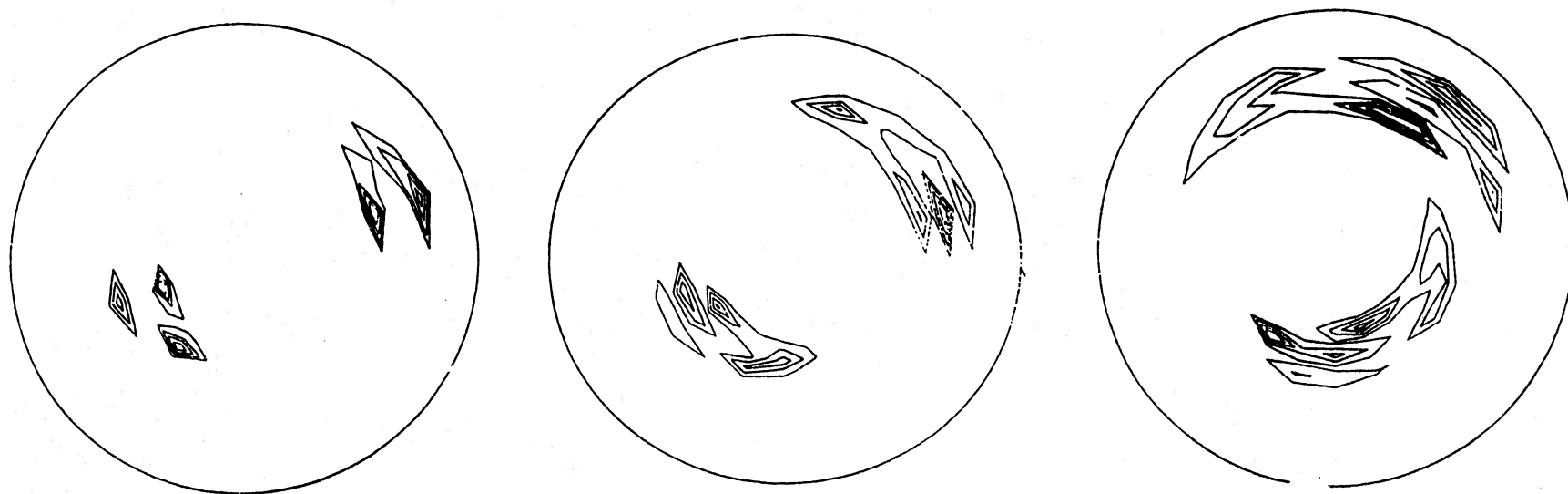
## VI. DISCUSSION AND SUMMARY

### a) Comparison with SSPSF Model

Our model resembles that of the SSPSF model in its fundamental viewpoint that the local physical process and its propagation make the global structure of a galaxy. The physical nature of trigger wave type is essentially the same as that of SSPSF. However, our method is quite different from that of SSPSF as compared in Table 1.

The most important distinction is the treatment of propagation. In SSPSF, all physical processes concerning the sequential star formation are absorbed into the uniform stimulating probability  $P_{st}$ , while they are expressed by the diffusion terms with uniform diffusion coefficients  $D_i$  in our model. In real galaxies, the intermediate of these two should be the case.

The SSPSF model has succeeded in getting irregular, patchy spiral arm structures which resemble those of M33, M101, etc. In old models (Seiden and Gerola 1982), these spiral structures were obtained only for a narrow range of the parameter  $P_{st}$  as far as the recovery time  $\tau$  of star-forming regions is not unphysically long ( $\tau \sim 10^8$  yr). This comes intrinsically from the stochastic nature like a “forest fire”



$t=42.5$

FIG. 10a

FIG. 10.—Effects of differential rotation on “Trigger Wave Type” structures. Contours of cold component ( $X_c = 0.3, 0.5, 0.7$ , and  $0.9$ ) are plotted for three cases of  $\Omega_1$ , i.e.,  $\Omega_1 = 0.019$  (*left*),  $0.062$  (*center*), and  $0.186$  (*right*). Parameters are the same as in Fig. 6. At  $t = 0$ , two different perturbations are set at nearly symmetric places with respect to the center. In the case of  $\Omega_1 = 0.062$ , irregular, patchy spiral arms of cold component are seen.



$t=145.0$

FIG. 10b



$t=270.0$

FIG. 10c



TABLE 1  
COMPARISON OF TWO MODELS

SSPSF	Our Model
Local physical process + propagation	Local physical process + propagation
Simulation of a stochastic process.	"Dissipative structures" by model equations.
Propagation by probability.	Propagation by diffusion.
Irregular, patchy spiral arms.	Three types of spatial structures including irregular, patchy spiral arms.
It is difficult to forecast the spatial patterns and not reproducible.	Spatial patterns can be forecasted and are reproducible.

(Seiden, Schulman, and Gerola 1979). However, by introducing the two-phase nature of interstellar gas, active and inactive for star formation, Seiden (1983) has succeeded in the formation of spiral structures for a wide range of  $P_{st}$ . Our spiral patterns, i.e., the "trigger wave type" structures, do not depend critically on the coefficients  $D_i$ , as is obviously seen.

Further, we have found two other qualitatively different mechanisms for the formation of spatial structures in galaxies, i.e., "symmetry breaking type" and "phase wave type." Because not only spiral arm structures, but also a variety of spatial structures, are found in real galaxies (Piddington 1973), we can imagine that some of them may be examples of "symmetry breaking type" or "phase wave type."

Another advantage of our method is that if the time structure of nonlinear reactions is known beforehand, we can forecast what type of spatial structures will appear.

#### b) Summary

Regarding a galaxy as an example of "dissipative systems," and analyzing model equations of ISM, we find three types of spatial structures are possible. We emphasize that a part of the structures of various galaxies can be understood by the concept of "dissipative structures."

It is noted that though our idea is essentially different from that of density wave theory, these two theories never conflict with each other. It seems that the gravitational potential may be important for the formation of some regular, grand design over a galaxy. However, such a regular structure is not common to all galaxies, and there are a plenty of galaxies which have irregular structures like bridges or filaments. In general, we may imagine that there are two competing mechanisms for the formation of spatial structures of a galaxy: one originates in the long-range gravitational force (density wave theory), and the other originates in the propagation of local phenomena ("dissipative structures"). The observations by Elmegreen and Elmegreen (1983) indicate that there are two distinct mechanisms for global spiral structure. This strengthens the above conjecture. Although we do not know why one of two mechanisms dominates in respective galaxies, we can grasp the diversity of structures in galaxies from this standpoint of view.

Apparently, the present model is too immature for comparing with realistic galaxies. We will present a further refined model in a succeeding paper.

We thank Professor S. Sakashita for his continuous encouragement. This research was supported in part by the Grant-in-Aid for Scientific Research Fund of the Ministry of Education, Science, and Culture (56540132).

#### REFERENCES

- Chevalier, R. A. 1974, *Ap. J.*, **188**, 501.  
 Cowie, L. L., and Rybicki, G. B. 1982, *Ap. J.*, **260**, 504.  
 Elmegreen, B. G., and Lada, C. J. 1977, *Ap. J.*, **214**, 725.  
 Elmegreen, D. M., and Elmegreen, B. G. 1983, preprint.  
 Field, G. B., Goldsmith, D. W., and Habing, H. J. 1969, *Ap. J. (Letters)*, **155**, L49.  
 Greenberg, J. M., Hassard, B. D., and Hastings, S. P. 1978, *Bull. Am. Math. Soc.*, **84**, 1296.  
 Habe, A., Ikeuchi, S., and Tanaka, D. Y. 1981, *Pub. Astr. Soc. Japan*, **33**, 23.  
 Hershkowitz-Kaufman, M., and Nicolis, G. 1972, *J. Chem. Phys.*, **56**, 1890.  
 Ikeuchi, S., Habe, A., and Tanaka, D. Y. 1984, *M.N.R.A.S.*, **206**, in press.  
 Ikeuchi, S., and Tomita, H. 1983, *Pub. Astr. Soc. Japan*, **35**, 77.  
 Kopell, N., and Howard, L. N. 1973, *Stud. Appl. Math.*, **52**, 291.  
 Landau, L. D., and Lifschitz, E. M. 1959, *Fluid Mechanics* (London: Pergamon).  
 Lin, C. C., and Shu, F. H. 1964, *Ap. J.*, **140**, 646.  
 Lin, C. C., Yuan, C., and Shu, F. H. 1969, *Ap. J.*, **155**, 721.  
 McKee, C. F., and Ostriker, J. P. 1977, *Ap. J.*, **218**, 148.  
 Minorsky, N. 1962, *Nonlinear Oscillations* (Princeton: Van Nostrand).  
 Nicolis, G., and Prigogine, I. 1977, *Self-Organization in Nonequilibrium Systems* (New York: John Wiley and Sons).  
 Ortoleva, P., and Ross, J. 1973, *J. Chem. Phys.*, **58**, 5673.  
 Piddington, J. H. 1973, *Ap. J.*, **179**, 755.  
 Roberts, W. W. 1969, *Ap. J.*, **158**, 123.  
 Seiden, P. E. 1983, *Ap. J.*, **266**, 555.  
 Seiden, P. E., and Gerola, H. 1982, *Fund. Cosm. Phys.*, **7**, 241.  
 Seiden, P. E., Schulman, L. S., and Gerola, H. 1979, *Ap. J.*, **232**, 702.  
 Shore, S. N. 1983, *Ap. J.*, **265**, 202.  
 Spitzer, L. 1962, *Physics of Fully Ionized Gases* (New York: Interscience).  
 Turing, A. M. 1952, *Phil. Trans. Roy. Soc. London*, **B 237**, 37.  
 Winfree, A. T. 1974a, *Sci. Am.*, **230**, No. 6, 82.  
 ———, 1974b, *Proc. SIAM-AMS Symp. Appl. Math.*, **8**, 13.  
 ———, 1978, *Theoret. Chem.*, **4**, 1.

SATORU IKEUCHI and TOSHIYA NOZAKURA: Department of Physics, Faculty of Science, Hokkaido University, Sapporo 060, Japan